Published in : Rapid Communications in Mass Spectrometry (2003), vol. 17, pp. 1847-1854.
Status : Preprint (Author's Version)

Thermometer ions for matrix-enhanced laser desorption/ ionization internal energy calibration

J.-F. Greisch[1], V. Gabelica[1], F. Remade[2] and E. De Pauw[1]

[1]Mass Spectrometry Laboratory, Liege University, 3 Allée de la Chimie Bat. B6c, B-4000 Liège, Belgium
[2]Theoretical Physical Chemistry Laboratory, Liège University, 3 Allée de la Chimie Bat. B6c, B-4000 Liège, Belgium

Abstract

This work describes a method to use relative fragmentation yields to characterize the internal energy distribution of ions produced by matrix-enhanced laser desorption/ionization mass spectrometry (MELDI-MS, see: Wright LG, Cooks RG, Wood KL. *Biomed. Mass Spectrom.* 1985; 12: 153-162). Assuming that the fragmentation proceeds statistically and that the collisions in the source lead to a Boltzmann-like distribution of the internal energy, a characteristic parameter, the effective temperature, is introduced to describe the internal energy distribution of the ions observed. The hypotheses, advantages and drawbacks of the implementation of the method that uses substituted benzylpyridinium salts as thermometer ions are discussed. Use is made of two matrices that produce no matrix cations in MELDI and are suitable for small cationic salts. The actual value of this effective temperature significantly depends on an accurate determination of the threshold dissociation energies and on the time spent in the source, in addition to the statistical hypothesis itself. The method could be applied to normalize spectra in order to compare results issued from different instruments.

In the present work, unusual matrices and analytes are studied to evaluate an approach that could be applied to access the internal energy distributions of analytes observed in matrix-assisted laser desorption/ionization (MALDI). The MALDI technique is widely used for mass spectrometric analysis of several types of non-volatile biomolecules, in particular peptides, proteins, oligonucleotides and oligosaccharides. Some understanding of its working mechanism has been gained;[4] however, it is not yet a fully understood technique. In the past few years several experimental approaches and theoretical models[12,20-24] have been under investigation to reach a better understanding of the mechanisms involved in the laser desorption and laser ionization processes relevant to MALDI mass spectrometry. The major experimental approaches consist of measurements of mean initial velocities of the analyte and matrix ions or neutrals,[2,3,5] study of proton transfer reactions and other chemical reactions,[30] and finally relative analysis of fragmentation reactions.[3,9,19]

Since few experimental data are currently available on the internal energies of MALDI ions, this paper aims to extend a method previously proposed by Collette and De Pauw in collaboration with Drahos and Vékey[10,11] for electrospray mass spectrometry. This method, when applied to matrix-enhanced/assisted laser desorption/ionization,[33] allows the direct characterization of the internal energy distribution of the observed analyte ions by means of a parameter having the dimension of a temperature. (Matrix-enhanced laser desorption/ionization, or MELDI, is a term applied when the matrix absorbs only weakly or negligibly at the laser wavelength.) The present results, obtained using unusual compounds, are intended to illustrate the applicability of the approach; other analytes and matrices, such as peptides and common matrices like α-cyano-4-hydroxycinnamic acid (CHCA) and 2,5-dihydroxybenzoic acid (DHB), will be investigated in the future and should help provide quantities more closely related to the MALDI process itself.

There is a major difference between the present approach and those of, e.g., Glückmann and Karas[2] or Berkenkamp, Hillenkamp and collaborators,[5] where the internal energy transferred to the analyte molecules is correlated to the initial velocities, the absorption cross-section, and the solid-state cohesion energy of the matrices. Indeed, the analysis discussed here provides, subject to validation of a few hypotheses, direct information on the energy distribution of the analyte ions observed.

An analysis following essentially the same reasoning as that discussed here and, like ours, based on the method proposed by De Pauw and collaborators for electrospray sources, has been proposed recently.[31] Although this work used the same substituted benzylpyridinium cations, it used different matrices and differs in the choice of the characteristic parameter. The choice of matrices and the characteristic parameter used in the present study are described below.

Published in : Rapid Communications in Mass Spectrometry (2003), vol. 17, pp. 1847-1854.
Status : Preprint (Author's Version)

The advantages and drawbacks of the use of benzylpyridinium cations as thermometer ions

The relative fragmentation yield method is implemented here using substituted benzylpyridinium salts. These compounds are those used in the previous similar analysis of the electrospray technique.[10,11] They present several advantageous properties and a few drawbacks if used for this purpose in MALDI-TOF experiments. These are discussed below.

Advantages

1. The main reason why the benzylpyridinium cations were initially chosen is that, under the conditions typical of electrospray, nano-electrospray and MALDI sources, they fragment by the rupture of a single bond, that between pyridine and benzyl. This allows use of a simple model for the fragmentation process, where the reaction coordinate is assumed to correspond to the elongation of the bond that breaks, without a reverse energy barrier.

2. Another advantage of the benzylpyridinium cations is that they are composed of a relatively small number of atoms. This allows *ab initio* computation of the physical quantities, such as the fragmentation threshold energies, and the vibrational frequencies of the reactant and transition states that are needed for calculation of the rate constants using the RRKM[26,27] statistical theory. Furthermore, the compounds studied are closed-shell cations that fragment into another closed-shell cation and a neutral pyridine, so that they may be computed at the restricted Hartree-Fock level.

Drawbacks

1. The major drawback of the use of substituted benzylpyri-diniums as thermometer ions is that the reactant and fragment ions have *m/z* values in the same range as fragments of the matrices commonly used in MALDI (CHCA and DHB, etc). For some substituted benzylpyridinium cations this may lead to uncertainty in the experimental values of the relative survival yields when these matrices are used. The matrices considered in the present work do not interfere with the analyte in this way.

2. The benzylpyridinium cations could undergo some fragmentation following their direct absorption of photons. Since the molecules embedded in the matrix are supposed to gain their internal energy from their matrix neighbours in the solid phase as well as from the collisions that occur in the plume, the contribution of photoinduced dissociation to the fragmentation yields will be neglected. The absorption of UV light by sodium nitrate and ammonium hydrogen carbonate, the matrices used here, is discussed below. Solid-phase UV-visible absorption of these two matrices was investigated, but no strong absorption bands were observed. There is however a matrix effect. Further justification can be found below. If photodissociation occurs, the quantities derived from the fragmentation of the benzylpyridinium cations would be dependent on the laser frequency and the transferability of these results to other compounds would be compromised.

3. The analyte ions detected constitute only a fraction of the analyte ions initially extracted from the plume, due to the fact that the ion optics of the instrument are not perfect. Consequently, an indirect hypothesis of the present method is that the experimental survival yields reflect a representative fraction of the plume and are thus not affected by the preferential loss of parent or fragment ions.

EXPERIMENTAL

Instrumentation

All experiments were performed using a Micromass Tof-Spec2E™ mass spectrometer in the positive ion reflectron time-of-flight (TOF) mode. The reflectron mode, due to an average resolution of 1300 in the *m/z* 100-220 range, allowed more accurate determination of peak intensities and thus fragmentation yields than was possible in linear mode. The nitrogen laser (model VSL 337i; Laser Science Inc., Cambridge, MA, USA) provides 4 ns pulses at 337 nm. The pulse energy of the laser is adjusted to 200 µJ resulting in a peak power of 50 kW. The fluence was varied coarsely by means of an orientable mirror and tuned by a diaphragm. Since no direct calibration of the laser fluence is possible on our instrument, the fluence will be defined by comparison with values of common use for peptides in common matrices. The fluence used for the sodium nitrate matrix corresponds approximately to twice the fluence used on the Tof-Spec2E™ for DHB. The value used for the ammonium hydrogen carbonate matrix is estimated to be equal to four times this value. For information, on the instrument used here, peptides are des-orbed from CHCA at a fluence half those required for DHB.

The source uses a one-step acceleration with delayed extraction; the delay before the extraction was 39 in arbitrary units. The ions were accelerated in an electric field corresponding to a source voltage of 20 kV, an extraction voltage of 20 kV, a focus voltage of 16 kV and a reflectron voltage of 26 kV. These values are as defined by Micromass. The pulse voltage was 2.8 kV and the detector voltage 1.85 kV. The vacuum before desorption was 3.4 x 10^{-3}Pa in the source and 1.7 x 10^{-4}Pa in the analyzer region.

The benzylpyridinium salts were synthesized and purified in this laboratory. The ammonium hydrogen carbonate and sodium nitrate matrices were purchased from Fluka Chemie AG (Buchs, Switzerland).

For each relative survival yield determined (see Table 2), about 25 values corresponding to different locations of the laser impact on the sample were averaged, and each of these values is the result of five laser shots on this same spot of the sample. Wherever specified, we use the sample standard deviation defined as:

$$\sigma = \sqrt{\frac{\sum_{i=1}^{n} (x_i - \bar{x})^2}{n-1}}.$$

Matrices

This work used ammonium hydrogen carbonate and sodium nitrate as matrices. These two matrices were chosen because they present no interferences in the mass spectra of small cationic compounds such as the benzylpyridinium salts. Therefore, they leave no doubt about the amount of fragment and parent ions detected since no ions due to the matrix occur at the *m/z* values corresponding to the analytes. This phenomenon can be explained by the emission of neutral preferentially to ionic species when these matrices decompose under laser irradiation.

Ionic crystals containing oxyanions, such as $NaNO_3$ and $CaCO_3$, were previously studied[6,28] and their laser-induced desorption is well known. The dominant mechanism for the laser-induced desorption of neutral species from surfaces in general involves thermal processes. The laser light is absorbed by the substrate, which undergoes rapid heating. The absorbate (sample) thus acquires thermal energy via thermally excited substrate lattice vibrations. The absorbate may then undergo various processes, including simple desorption from the surface.[6] However, for ionic crystals containing oxyanions, non-thermal mechanisms appear to play a significant role.[6,7] At low fluences (<80mJ/cm^2), the main neutral product following UV laser light irradiation of $NaNO_3$ is NO accompanying NO_3^- dissociation. The NO emission is strongly increased if the surface has a high number of defects. These defects can be produced by laser impact[7] or by the inclusion of an analyte. Similar behaviour is observed for calcite during UV irradiation, with CO emitted.[8] In the case of ammonium hydrogen carbonate, used here as a matrix, similar behaviour is assumed. However, this compound also decomposes by heating above 35°C producing ammonia gas, carbon dioxide, and water vapour. The decomposition of ammonium hydrogen carbonate and sodium nitrate upon UV irradiation will be discussed further below.

Examples of spectra obtained using ammonium hydrogen carbonate (Fig. 1) and sodium nitrate (Fig. 2) as matrices are presented for the *p*-chlorobenzylpyridinium cation. No interferences are observed. The samples were crystallized under vacuum, producing a rather homogeneous crystallization. The laser energy necessary to detect analyte ions is above the threshold for the matrices commonly used in MALDI analysis of analytes such as peptides. However, since for technical reasons it is not possible to determine for our spectrometer the exact amount of energy received per square centimeter during the laser excitation, the fluence values used were compared above with those for common MALDI matrices.

The matrix solution was prepared in 1:1 acetonitrile/ water, similar to the benzylpyridinium solution. The matrix and analyte were mixed before deposition on the target plate, and were co-crystallized under vacuum using the dried-droplet method. The matrix-to-analyte ratio in the sample was approximately 2500:1; this was optimized to avoid saturation and give more reliable survival yields.

Figure 1. *MELDI mass spectrum of p-CI-benzylpyridinium cation with ammonium hydrogen carbonate as matrix. The p-Cl-benzyl fragment is observed at m/z 125, and the parent ion at m/z 204. Note the CI isotope peaks and the absence of matrix peaks.*

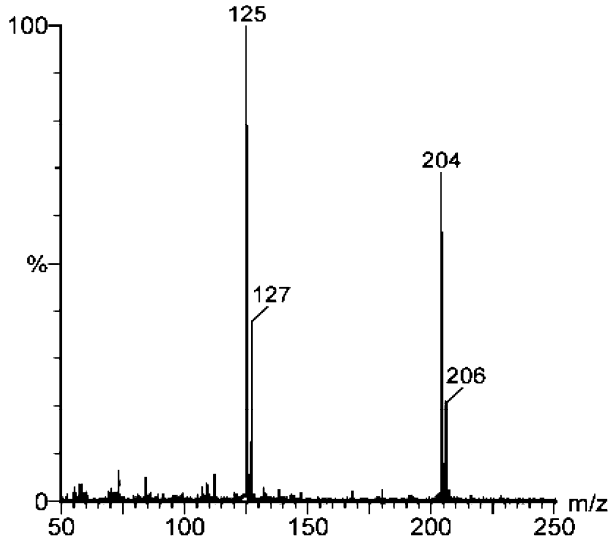

Figure 2. *MELDI mass spectrum of p-CI-benzylpyridinium cation with sodium nitrate as matrix. Compare Fig. 1.*

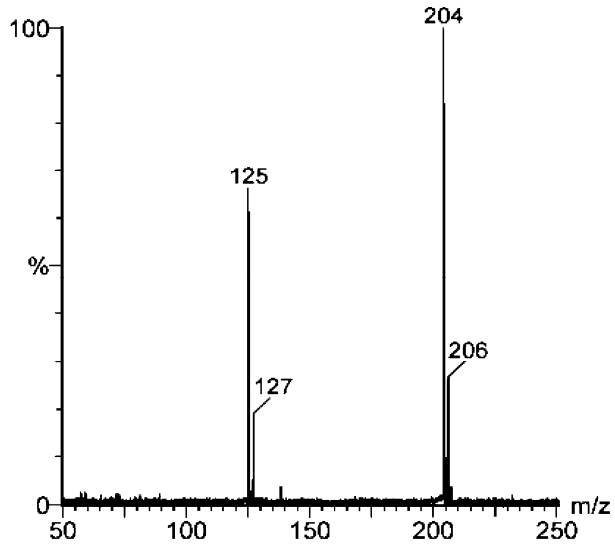

MODEL OF THE FRAGMENTATION MECHANISM

The description of the internal energy distribution of the observed analyte ions, applied in this work, relies on the assumption that the single bond fragmentation proceeds statistically. We assume that the internal energy is redistributed statistically over the normal modes. We assume furthermore that the internal energy distribution of a set of molecules is Boltzmann-like. The internal energy of the benzylpyridinium cations is the result of several contributions, e.g., the vibrational excitation of the matrix prior to the ejection of the molecules forming the plume, the collisions in the gas phase, etc. At this stage we do not know how important the several contributions are. However the Boltzmann-like internal energy distribution hypothesis is sustained by the number of collisions occurring in the plume. Indeed, it was shown by Vertes[12-14] in a theoretical treatment of the plume dynamics that, for experimental conditions similar to those characteristic of MALDI-MS, the plume density is sufficient to lead to a multiple collision activation/deactivation mechanism. The number of collisions that would lead to an exact Boltzmann distribution is not known since we do not have information on the internal energy prior to the

collisions. However, if the results obtained by Laskin and Futrell[34] for sustained off-resonance excitation in a Fourier transform ion cyclotron resonance mass spectrometer can be assumed to be transferable to MALDI conditions, the average energy transferred upon collisions reaches a stationary state at between 15-20 collisions. This small number of collisions may thus be enough to justify the Boltzmann-like hypothesis.

The statistical hypothesis also allows the use of the RRKM theory[26,27] to compute the microcanonical dissociation rate constant; no account will be taken of the conservation of the total angular momentum in our computations. The model, developed by Drahos *et al.,*[11] is now briefly outlined. As discussed above, the distribution of the internal energies of the emitted ions is modeled by a Boltzmann-like distribution, which allows determination of an internal effective temperature.[1] At this stage, one must regard this temperature only as a parameter describing the distribution of internal energy of an ion population. The relationships giving the survival fraction of parent ions follow treatments given in Refs. 26 and 27.

For a population of molecules subjected to collisional activation, the assumption of a Boltzmann-like distribution of the excitation energy amounts to definition of a temperature T, and the fraction of molecules with internal energy £ is given by:

$$P(E,T) = \frac{\rho(E)e^{-E/k_BT}}{\int_0^\infty \rho(E)e^{-E/k_BT}\,\mathrm{d}E} \qquad (1)$$

where k_B is the Boltzmann constant and ρ(E) the microcanonical density of states at energy E. The reaction of a benzyl-pyridinium ion at a given total internal energy E is now considered:

$$[BenPyr^+](E) \xrightarrow{k(E)} products \qquad (2)$$

The reaction rate is given by:

$$-\frac{\mathrm{d}[BenPyr^+](E)}{\mathrm{d}t} = k(E)[BenPyr^+](E) \qquad (3)$$

where *k(E)* is the unimolecular microcanonical rate constant. Under the statistical assumption discussed above, *k(E)* can be estimated using the RRKM theory[26,27] and takes the form:

$$k(E) = \frac{N^{\ddagger}(E-E_0)}{h\rho(E)} \qquad (4)$$

where E is the excitation energy and E_0 the threshold energy. N* (E -E_0) is the number of states of the transition state for the excess energy (E - E_0) and ρ(E) the density of states of the reactants; h is the Planck constant. The concentration of parent ions at the energy E and at time τ is derived by integration of Eqn. (3):

$$[BenPyr^+](E,\tau) = [BenPyr^+](E,0)e^{-k(E)\tau} \qquad (5)$$

where τ is the time interval during which the dissociation is observed.

It is possible to consider two different observation times for the parent and fragment ions. This is relevant if, for ion optics reasons, a fraction of the parent ions extracted is undetected, or if some of the fragmented ions are detected as non-fragmented ones. In this work, we consider the same observation time for the parent and fragment ions: $\tau = \tau_1 = \tau_2$.

The fraction of ions of internal energy E at time τ — 0 is equal to:

$$[BenPyr^+](E,0) = [BenPyr^+](0)P(E,T) \qquad (6)$$

The populations of the parent cation and the fragment ion at time τ are given by:

$$I_{\mathrm{Ben}^+}(T) = \int_0^\infty P(E,T)\left[1 - e^{-k(E)\tau}\right] \mathrm{d}E \tag{7}$$

$$I_{\mathrm{Ben}^+\mathrm{Pyr}}(T) = \int_0^\infty P(E,T)\left[e^{-k(E)\tau}\right] \mathrm{d}E \tag{8}$$

The fraction of surviving parent ions at time τ is:

$$Y^{\mathrm{calc}}(T) = \frac{I_{\mathrm{BenPyr}^+}(T)}{I_{\mathrm{BenPyr}^+}(T) + I_{\mathrm{Ben}^+}(T)} = \int_0^\infty P(E,T) e^{-k(E)\tau} \mathrm{d}E \tag{9}$$

and is fitted to the observed experimental value by varying the effective temperature parameter *T*. Using the theoretical internal energy distribution thus determined, it is possible to derive a mean internal energy associated with the measured survival yields:

$$E_{\mathrm{mean}} = \int_0^\infty P(E,T) E \, \mathrm{d}E \tag{10}$$

This mean energy differs from that determined in Ref. 31, where an effective internal energy is extracted by solving numerically the relationship:

$$k_{\mathrm{exp}} = -(1/\tau)\ln(Y_{\mathrm{exp}}) = k_{RRKM}(E)|_{E_{\mathrm{eff}}}$$

where Y_{exp} is the experimental survival yield defined in Eqn. (9), and τ is the reaction time in the accelerating region, similar to our fragmentation time window detailed further below. E_{eff} corresponds to the unique internal energy giving the same theoretical survival yield as the measured value. In this paper we assume a Boltzmann-like internal energy distribution; the fitting parameter of the internal energy distribution is the effective temperature (*T*).

In order to obtain Y^{calc} (T), the RRKM rate constant (Eqn. (4)) has to be calculated and the time interval τ for the mass spectrometer estimated. The RRKM rate constant depends on the vibrational frequencies of the benzylpyridinium cation at the equilibrium reactant state and at the transition state geometry, and also on the threshold energy E_0. These parameters were obtained by SCF *ab initio* computations for the parent and the fragment ions using the GAMESS-US program[15] with a 6-31G* basis set. The determination of the vibrational frequencies at the equilibrium configuration is straightforward. As discussed in the Introduction, it is assumed that the reaction coordinate is given in good approximation by the elongation of the C-N bond between the Ben and Pyr fragments and that there is no reverse barrier along it, the fragmentation occurring by simple bond cleavage. The vibrational frequencies of the transition state were therefore estimated by interpolation between those of the parent and the fragment ions. Further checks were made to ensure that use of slightly different sets of frequencies for the transition state does not affect significantly the computed effective temperature.

The effective temperature depends more significantly on the value of the critical energy E_0 that is used. The thresholdenergies E_0 were computed at the same level of *ab initio* computation. They are 10-15% higher than values taken from the literature[16,17] and previously used by our group, but the SCF level is known to overestimate dissociation energies.[29] Larger dissociation energies lead to somewhat higher effective temperatures, as discussed below. The choice of the basis set 6-31G* and calculation technique is justified by the fact that they provide, for the compounds for which the comparison was made, the correct relative stabilities.[32]

The last parameter, the fragmentation time window, τ, is determined using the ion optics simulation software Simion 3D.[18] We estimated the fragmentation time window as 3.2 μs; the impact of the fragmentation time window on the effective temperatures and mean energies is discussed below. The initial velocities were taken to be of the same order of magnitude as those determined by Ghickmann and Karas.[2] The trajectories of the ions

were modeled using information given by the manufacturer of the mass spectrometer.

The results described in the next section are based on the further assumption that no post-source decay takes place, or that it is negligible. Indeed we have experimental evidence that, in our case, the percentage of metastable ions is quite small. This could be due to the fact that the plume expansion mechanism leads to the deactivation of the molecules before they enter the field-free region of the TOF mass spectrometer. The fragmentation time windows used here take into account the delay before the extraction pulse. However, since these times are the result of a modeling in which the initial velocities have been estimated, and since there is some uncertainty about the region of the source where the fragmentation occurs, we investigated the influence of the fragmentation time window (parameter τ) on the effective temperature (Fig. 4); these results are discussed below.

RESULTS

A two-step acquisition procedure was used for both matrices. The first five laser shots were averaged as well as the next five, to allow background elimination and derivation of reliable relative intensities of the parent and fragment ions. For each substituted benzylpyridinium cation about 25 experimental survival yields were collected. From these yields, the corresponding effective temperatures and mean energies were calculated using the method outlined above; two central hypotheses are made, namely, that the fragmentation proceeds statistically and that the internal energy distribution is Boltzmann-like.

The parameters required for the determination of the effective temperature are the frequencies of the equilibrium reactant and transition state of the molecules studied, the fragmentation threshold energy, and the fragmentation time window. The first two were determined by *ab initio* calculations for the parent and fragment ions. Since a simple bond cleavage between the pyridine and the benzyl cation is the only reaction observed, it is likely that there is no reverse activation barrier. The frequencies of the transition state were therefore determined from a comparison of the frequencies of the fragment and parent ions. As the RRKM reaction rate is rather robust with respect to small differences in the frequencies, the errors in the frequencies can be regarded as responsible for only negligible errors in the effective temperatures and mean energies. The two most important factors are the fragmentation threshold energy (E_0) and the fragmentation time window (τ). The value of E_0 was derived from the difference between the total energies of the parent and fragment ions.

The survival yields measured for the benzylpyridinium cations, using ammonium hydrogen carbonate and sodium nitrate as matrices, are presented in Fig. 3. For each matrix the survival yields are plotted for both the five first laser shots and for the next five laser shots on the same set of locations of the sample. For the ammonium hydrogen carbonate matrix, the survival yields for the first five laser shots are lower than for the second set of laser shots. A possible explanation could be related to the decomposition of this matrix. As mentioned above, both the thermal processes and the presence of defects generated by previous laser shots are responsible for the laser-induced desorption of the matrix. The mechanisms and reactions occurring could provide an explanation for this softer desorption since the matrix would have accumulated energy and defects from the previous shots and would thus decompose more easily. For the sodium nitrate no noticeable difference is observed between the two sets of laser shots. The fact that the survival yields do not decrease upon increased laser irradiation leads to the conclusion that there is a matrix effect operating.

From the measured survival yields, effective temperatures can be extracted. We first discuss the influence of the fragmentation time window and of the fragmentation threshold energy on these temperatures.

The effect on the effective temperatures of the uncertainty in the fragmentation time window is illustrated in Fig. 4, which shows effective temperatures calculated for different values of the fragmentation time window. A similar dependence on the fragmentation time window is observed for the mean internal energies. If a shorter fragmentation time window than the estimated value is considered, the derived effective temperatures and mean energies will be shifted upwards, leaving the other figures (Figs. 5 and 6) otherwise unchanged. Our best estimate of the fragmentation time window was 3.2 μs. This value was obtained, using the limited amount of information available about the ion source of our mass spectrometer, using the ion optics software SIMION; it can be regarded as a fixed value used for comparison purposes.

The effect on the effective temperature of the error in the determination of the fragmentation threshold energy is illustrated in Table 1 for the *p*-methylbenzylpyridinium ion. The fragmentation time window was taken to be 3.2 μs. Different values of the fragmentation threshold energy, centered on 1.80eV (the value given by the *ab initio* calculation), were considered.

For a given internal energy distribution, a higher fragmentation threshold energy leads to a lower value of the numerator N* (E—E_0) in Eqn. (4). Therefore, for a fragmentation to be observed within the instrument time window, the internal energy distribution needs to be shifted to higher values.[25] In the same way, in order to get the same survival yield, a longer fragmentation time window causes the internal energy distribution to be shifted to lower energies. From this point on we consider the fragmentation time window to be the estimated value of 3.2 µs, and the fragmentation threshold energies considered are those obtained by *ab initio* calculations. The effective temperatures and the mean energies, derived from the experimental survival yields, as well as their respective standard deviations for both matrices and both sets of shots, are presented in Table 2.

Figure 3. *Comparison of the survival yields for NH_4HCO_3 and $NaNO_3$.Experimental fragmentation yields measured for the different benzylpyridinium cations and for both matrices studied. Two sets of values are considered, for the five first and the next five laser shots on the same set of locations on the sample. The bars correspond to the standard deviations from the mean. The benzylpyridinium cations are characterized by their fragmentation threshold energies, E_0.*

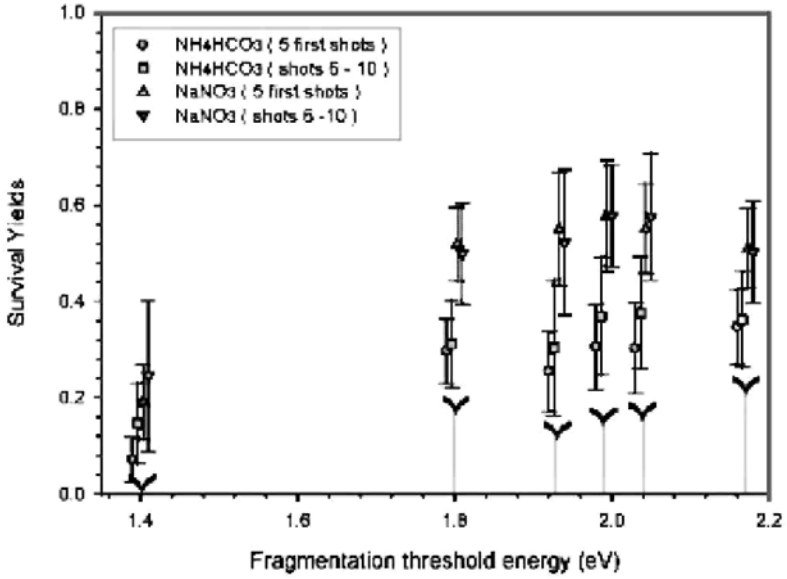

Figure 4. *NH_4HCO_3 used as matrix (5 first shots). Effect of the uncertainty in the estimated fragmentation time window on the effective temperature. The lower values of the fragmentation time window considered correspond to hypothetical values of the time spent in the high-density region of the mass spectrometer, which approximately extends over the source. The intermediate values correspond to the times during which the fragmentation may occur. The higher values correspond to the time needed for the ions to enter the reflectron, be reflected, and reach the detector; these latter values are given for reference purposes only. The value estimated using SIMION, relevant to the present work, is 3.2 µs.*

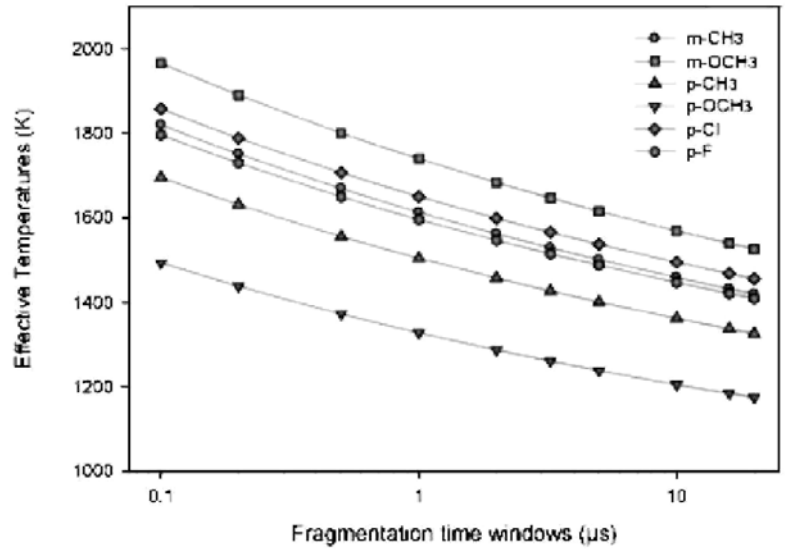

Published in : Rapid Communications in Mass Spectrometry (2003), vol. 17, pp. 1847-1854.
Status : Preprint (Author's Version)

Figure 5. *Comparison of the effective temperatures for NH_4HCO_3 and $NaNO_3$. The effective temperatures corresponding to the internal energy distributions determined for the benzylpyr-idinium cations for both matrices. Two sets of values are considered, for the five first and the next five laser shots on the same set of locations on the sample. The bars correspond to the standard deviations from the mean.*

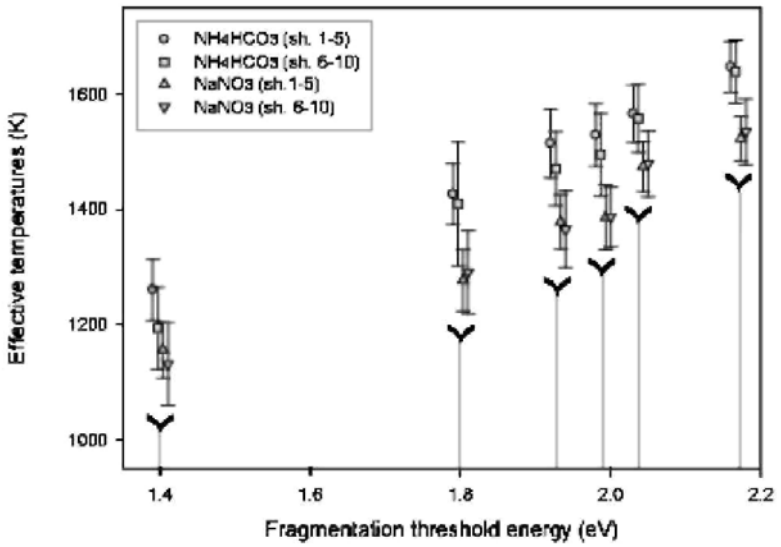

Figure 6. *Comparison of the mean energy for NH_4HCO_3 and $NaNO_3$. The mean energies corresponding to the internal energy distributions determined for the benzylpyridinium cations. The mean energies are determined for each substituted benzylpyridinium cation and for both matrices. Two sets of values are considered, for the five first and the next five laser shots on the same set of locations on the sample. The bars correspond to the standard deviations from the mean. The benzylpyridinium cations are characterized by their fragmentation threshold energies.*

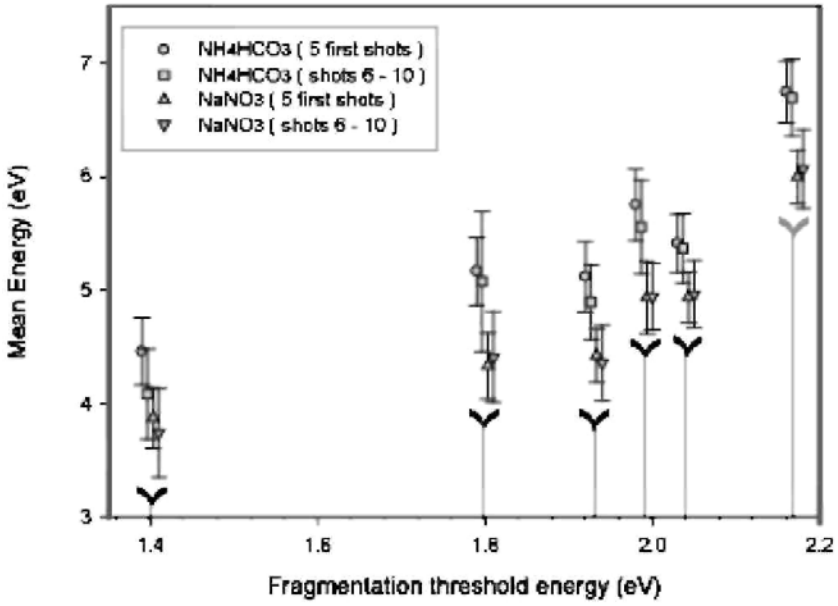

Table 1. *Effect of the uncertainty in the determination of the fragmentation threshold energy on the effective temperature. This simulation is made for the p-methylbenzylpyridinium cation. The estimated time window used is τ = 3.2 μs, and the survival ratio considered is 0.5. Different values of the fragmentation threshold energy, centered on the calculated value 1.80eV, are explored*

Surv. yield	E_0 (eV)	T_{eff} (K)	E_{mean}(eV)
0.5	1.60	1165	3.73
0.5	1.70	1232	4.09
0.5	1.80	1299	4.45
0.5	1.90	1365	4.82
0.5	2.00	1432	5.19

Table 2. *Effective temperatures and mean energies of the substituted benzylpyridinium cations (all six values are averaged) for the first and second sets of five laser shots on different locations of the sample, using ammonium hydrogen carbonate and sodium nitrate as matrices. The estimated fragmentation time window is 3.2 μs*

Matrix	T_{eff} (K)	σ(T_{eff}) (K)	*E*mean (eV)	σ(E_{mean}) (K)
$NaN0_3$1st set of laser shots	1366	133	4.75	0.73
$NaN0_3$ 2nd set of laser shots	1364	142	4.75	0.79
NH4CO3 1st set of laser shots	1490	133	5.44	0.77
$NH_4C0_3$2ndset of laser shots	1460	153	5.28	0.86

For the sodium nitrate matrix, the values obtained for the two sets of laser shots are identical; this can be seen in more detail in Figs. 5 and 6, where the standard deviation bars completely overlap. The average of the six effective temperature values thus has a standard deviation equal to 9.7% of the average value, and the average mean energy a standard deviation equal to 15.4% of the average value.

Considering now the values obtained for the different benzylpyridinium cations in the ammonium hydrogen carbonate matrix, even if the survival yields appear to be higher for the second set of five laser shots, the effective temperatures and mean energies are of the same order of magnitude and well within the uncertainty range around the averages. The average of the six effective temperature values has a standard deviation equal to 8.9% of the average value, and the average mean energy a standard deviation equal to 14.0% of the average value for the first set of five laser shots.

The survival yields are higher for the sodium nitrate matrix. Thus, sodium nitrate transfers less energy to the sample than the ammonium hydrogen carbonate matrix. For both matrices, for a given substituent, the standard deviation is about 4% of the effective temperature average except for the *p*-methoxybenzylpyridinium cation. If we consider the standard deviation of the effective temperature averages obtained for the six different benzylpyridinium cations, it is about 10% of the value of the mean. This allows the conclusion that the effective temperatures describe a phenomenon common to the different cations. This is all the more true as the *p*-methoxybenzylpyridinium cation is excluded from the averages of the various benzylpyridinium cations, since it

presents for both matrices a higher survival yield than could have been expected. A possible explanation could be the underestimation of the number of fragments due to a possible second-generation fragmentation involving the loss of OCH_3 or CH_3 and thus an overestimation of the survival yields. Were the survival yields of the p-OCH_3 ion lower, its effective temperatures would be higher and the standard deviation on these even smaller.

From experiments made with CHCA as matrix (not detailed here and described briefly for reference purposes), mean effective temperatures were obtained in the range 1050-1300 K, depending on the sample preparation method. For this matrix the solvent used and the evaporation conditions strongly affect the crystal formation and the energy transferred to the sample upon laser desorption. As explained above, there may also be an uncertainty in the intensities measured for this matrix as some of the matrix ions are detected at the same mass-to-charge ratio as several of the cations of interest. A new family of thermometer compounds is being tested that could be used with matrices like CHCA and DHB. This new family of compounds will also provide a check on the statistical hypothesis.

CONCLUSIONS

The present work explores further the use of fragmentation yields to access the internal energy distributions of ions produced by matrix-enhanced/assisted laser desorption/ionization. The method, similar to that used previously to characterize the experimental conditions in electrospray sources, was implemented using benzylpyridinium salts as the analytes. Their simple fragmentation mechanism makes these compounds prime candidates for such a study. Two matrices, ammonium hydrogen carbonate and sodium nitrate, suitable for the study of small cationic compounds such as the benzylpyridiniums, were investigated. Their advantage is that they do not emit positive ions in positive ion MALDI-TOFMS. This is of particular interest for the present study since some of the ions studied have the same *m/z* ratio as fragments of commonly used matrices (e.g., CHCA, DHB) which can cause some uncertainty in the survival yields.

From the experimental survival yields, effective temperatures characterizing the internal energy distribution of a population of ions emitted by matrix-enhanced laser deso-rption/ionization were determined. For the six benzylpyr-idine cations studied, an average effective temperature of 1460 K with a standard deviation of 153 K was obtained for the ammonium hydrogen matrix, whereas an average effective temperature of 1366 K with a standard deviation also of 133 K was obtained for the sodium nitrate matrix. For a given substituent on the benzyl group, the value of the effective temperature depends on the assumed values of fragmentation threshold energy and the fragmentation time window. For a given substituent the standard deviation is about 5% of the effective temperature average. The standard deviation of the effective temperature averages obtained for the six different benzylpyridinium ions is about 10% of the value of the mean.

To conclude, insofar as a reliable estimation of the fragmentation threshold energy and fragmentation time window can be made, it is possible to characterize the effect of the experimental conditions on the internal energy distribution by an effective temperature. Compounds presenting a different ionization mechanism, such as protonation, could provide further insight into the mechanisms involved.

REFERENCES

1. Ervin KM. *Int. J. Mass Spectrom.* 2000; 195/196: 271.

2. Glückmann M, Karas M. *J. Mass Spectrom.* 1999; 34: 467.

3. Stevenson E, Breuker K, Zenobi R. *J. Mass Spectrom.* 2000; 35: 1035.

4. Zenobi R, Knochenmuss R. *Mass Spectrom. Rev.* 1998; 17: 337.

5. Berkenkamp S, Menzel C, Hillenkamp F, Dreisewerd K. *J. Am. Soc. Mass Spectrom.* 2002; 13: 209.

6. *Low Fluence Laser Desorption and Plume Formation from Wide Bandgap Crystalline Material, Laser Ablation and Desorption,* Miller JC, Haglund RF (eds). Experimental Methods in the Physical Sciences, vol. 30. Academic Press, 1998; 139-172.

7. Webb RL, Langford SC, Dickinson JT. *Nucl. Instr. Methods Phys. Res. B* 1995; 103: 297.

8. Beck KM, Taylor DP, Hess WP. *Phys. Rev. B* 1997; 55:13253.

9. Spengler B, Kirsch D, Kaufmann R. *J. Phys. Chem.* 1992; 96: 9678.

10. Collette C, De Pauw E. *Rapid Commun. Mass Spectrom.* 1998; 12: 165.

11. Drahos L, Heeren RM, Collette C, De Pauw E, Vékey K. *J. Mass Spectrom.* 1999; 34: 1373.

12. Vertes A, Juhasz P, De Wolf M, Gijbels R. *Int. J. Mass Spectrom.* 1989; 94: 63.

13. Balazs L, Gijbels R, Vertes A. *Anal. Chem.* 1991; 63: 314.

14. Vertes A, Irinyi G. *Anal. Chem.* 1993; 65: 2389.

15. GAMESS-US Version 26 Oct 2000, R3 from Iowa State University Schimdt MW, Baldridge KK, Boatz JA, Elbert ST, Gordon MS, Jensen JH, Koseki S, Matsunaga N, Nguyen KA, Su SJ, Windus TL, together with Dupuis M, Montgomery JA. *J. Comput. Chem.* 1993; 14: 1347, Silicon Graphics version.

16. Collette C, Drahos L, De Pauw E, Vékey K. *Rapid Commun. Mass Spectrom.* 1998; 12: 1673.

17. Katritzky AR, Watson CH, Dega-Szafran Z, Eyler J. *J. Am. Chem. Soc.* 1990; 112: 2471.

18. Dahl DA. SIMION 3D version 6.0, *Proc. 43rd ASMS Conference Mass Spectrometry and Allied Topics,* May 21-26, Atlanta, GA, 1995; 717.

19. Karas M, Bahr U, Strupat K, Hillenkamp F, Tsarbopoulos A, Pramanik BN. *Anal. Chem.* 1995; 67: 675.

20. Johnson RE. *Int. J. Mass Spectrom. Ion Processes* 1994; 139: 25.

21. Knochenmuss R. *J. Mass Spectrom.* 2002; 37: 867.

22. Knochenmuss R, Stortelder A, Breuker K, Zenobi R. *J. Mass Spectrom.* 2000; 35: 1237.

23. Horneffer V, Forsmann A, Strupat K, Hillenkamp F, Kubitscheck U. *Anal. Chem.* 2001; 73: 1016.

24. Zhigilei LV, Kodali PBS, Garrison BJ. *J. Phys. Chem. B* 1997; 101: 2028.

25. Lifshitz C. *J. Phys. Chem.* 1982; 86: 606.

26. Baer T, Hase WL. *Unimolecular Reaction Dynamics: Theory and Experiments,* Oxford University Press: Oxford, 1996.

27. Steinfeld JI, Fransisco JS, Hase WL. *Chemical Kinetics and Dynamics.* Prentice Hall: Upper Saddle River, 1999.

28. Li YCL, Cheng S, Chan D. *Rapid Commun. Mass Spectrom.* 1998; 12: 993.

29. Scott AP, Radom L. *J. Phys. Chem.* 1996; 100: 16502.

30. Mowry CD, Johnston MV. *J. Phys. Chem.* 1994; 98: 1904.

31. Luo G, Marginean I, Vertes A. *Anal. Chem.* 2002; 74: 6185.

32. Csonka GI. *J. Mol. Struct.* 2002; 584: 1.

33. Wright LG, Cooks RG, Wood KL. *Biomed. Mass Spectrom.* 1985; 12: 153.

34. Laskin J, Futrell J. *J. Phys. Chem.* 2000; 104: 5484.